Iorio, M., Teno, J., Nicolás, M., García-González, R., Peláez, V. H., González-Gaitano, G. & González-Benito, J. (2018). Conformational changes on PMMA induced by the presence of TiO2 nanoparticles and the processing by Solution Blow Spinning. *Colloid and Polymer Science, 296*(3), pp. 461–469.

DOI: 10.1007/s00396-018-4268-0

Conformational Changes on PMMA Induced by the Presence of TiO_2 Nanoparticles and the Processing

M. Iorio[1,2], J. Teno, M. Nicolás[1], R. García-González[1], V.H. Peláez[1], G. González-Gaitano[3], J. González-Benito[1]

[1]*Dept. Materials Science and Engineering and Chemical Engineering, IQMAAB, Universidad Carlos III de Madrid, Madrid, Spain*

[2]*Dpt. Chemical Engineering and Materials, Sapienza-Università di Roma, Rome, Italy*

[3]*Dept. Química, Facultad de Ciencias, Universidad de Navarra, 31080, Pamplona, SPAIN*

Abstract

Poly(methylmethacrylate), PMMA, films filled with titanium oxide, TiO_2, nanoparticles were prepared by solution blow spinning, SBS. The influence of the presence of nanoparticles in the physicochemical properties of the material was studied. The PMMA/TiO_2 nanocomposites with different amounts of TiO_2 (up to 10% by weight) were prepared in the form of films by SBS using a commercial airbrush. Morphology, structure and thermal properties were studied by scanning electron microscopy (SEM), Fourier transformed infrared spectroscopy (FTIR), thermogravimetry (TGA), and differential scanning calorimetry (DSC). It was demonstrated that SBS allowed obtaining PMMA/TiO_2 nanocomposites with a relatively high amount of nanoparticles uniformly dispersed within the polymeric matrix. All results point out that the macromolecular flow, forced by the SBS process, so as the specific interactions and the TiO_2 surface induce a preferential conformation of the ester group respect to the PMMA backbone, at least when the number of aggregates low enough.

Keywords: PMMA, solution blow spinning, nanocomposites, characterization.

1. Introduction

It is very well known that a wide range of properties can be tailored by the simple way of mixing different materials for which at least one of them had nanoscale dimensions. Among the different possibilities, polymers filled with different nanoparticles are very promising materials since, in many cases, apart from the easy procesability they present unique properties, such as the ones required for several specific applications like electrical or magnetic shielding or UV resistance [1–6], and coatings or adhesives with reduced coefficient of thermal expansion [7, 8]. In general, these particular properties are due to the presence of the nanoparticles, where the polymer is acting as the matrix (also with its own properties) in which those particles are dispersed which, in addition, provides, in general, more consistency to the material.

In general terms, these properties (sometimes improved ones and some other unique ones) can only be obtained if there is an adequate dispersion of the nanoparticles within the polymer matrix. It is generally accepted that mixtures of organic polymers with inorganic nanoparticles lead to a phase separation with agglomeration of particles which will be translated into poor optical and mechanical properties. For this reason, several methods have been used in order to get good dispersions of nanoparticles in polymeric matrices [9]. However, at least when the particle size is lower than 50 nm, it is very difficult to obtain homogeneous mixtures (not in a thermodynamical sense but in terms of dispersion of particles) if the amount of filler is higher than 5% by weight or if the viscosity of the melt polymer is very high. Therefore, it is very important to find out and develop new processing methods to carry out these requirements.

Several methods have been tried to obtain uniform nanoparticle dispersions within polymer matrices; however, most of them require long processing times, chemical modification of the matrix and/or the filler, and even sometimes high processing temperatures [10–14]. González-Benito et al. have used high-energy ball milling (HEBM) as a method to mix a polymer with inorganic nanoparticles in the solid state, achieving an extraordinary dispersion of nanoparticles within the polymer [7, 9, 15–21]. However, this method is usually time consuming and, for certain polymers, chain scission may occur [21].

To overcome some of these drawbacks, the use of solution blow spinning, SBS, can be a promising method. With SBS, developed by Medeiros et al., the spinning is carried out with a device formed by concentric nozzles through which a polymer solution is ejected by the action of pressurized gas. In this way it is possible to produce, depending on the conditions from flat films to micro- and nanofibers of several thermoplastics [22]. Recently, Costa et al. [23] and González-Benito et al. [24] have described the preparation of nanocomposites with SBS. The nanoparticles fly with the polymer during the ejection process in some way that when impacting the collector they do it together allowing a good dispersion of nanoparticles within the polymer [24].

In the field of nanocomposites it is important to highlight that, due to its low size, nanoparticles present a high surface to volume ratio, leading to high energy surfaces. One of the most desirable results when mixing nanoparticles with a polymer is to increase as much as possible the adhesion between both components. The classical theories of composite materials predict that an improvement of the adhesion between the polymer matrix and the phase which is acting as the reinforcement yields an

improvement of the mechanical properties [17, 18].These theories are based on the idea that the modulus of a composite is a function of its constituents volume fraction, the shape and the ordering of the particles and the interphase formed between the polymer matrix and the particles. The structure of the interphase differs depending on the reinforcement and the polymer matrix and, in general terms, it varies with the distance from the surface of the particles. Due to these differences in the structure, the properties of the polymer in the interphase can be very different from those in the bulk, which is an important factor that greatly affects the effectiveness of the load transfer between the polymer matrix and the reinforcement. In particular, in the case of nanocomposite materials and considering the high specific area of the nanoparticles, the interfacial properties can even be the predominant factor affecting the final properties of the nanocomposite. For instance, by simple calculations based on geometric considerations it is possible to estimate that one interphase of only 1 nm thick surrounding the nanoparticles can be an important volume fraction of the overall material (more than 30 %).

At this point it seems opportune to take a further step by performing studies in polymers filled with dispersed nanoparticles using new methods of nanofiller dispersion, like SBS, with the objective of investigating the influence of the nanofiller in the composite behaviour and understand their relation with the final properties of the nanomaterial. Recently, González-Benito et al. have used SBS as a method to mix polysulfone [24], PSF, and polyvinylidene fluoride [25], PVDF, with polymer TiO_2 nanoparticles achieving an good dispersion of the nanoparticles within the polymer. However, it is not clear yet what is the effect that this procedure can provoke in the polymeric structure and what kind of adhesion is achieved between the nanoparticles and the polymer.

In this work, a PMMA filled with TiO_2 nanoparticles prepared by SBS was selected as nanocomposite and the influence of the presence of nanoparticles so as the processing used on some of the physicochemical properties of the polymer was studied. Although the composition of the nanoparticles might affect the final properties of the nanocomposites, as was stated by Motaung et al. [26, 27], the use of this TiO_2 nanopowder has not other intention than using them as nanoparticles, with potential interesting properties such us antimicrobial, optical, etc., to be inserted within a conventional polymer, using SBS to get a uniform dispersion which facilitates the interpretation of the final properties of the nanocomposites.

2. Experimental part

2.1. Materials

Polymethylmethacrylate, PMMA, (M_w = 25000 g/mol, Polysciences, Inc.) was used as the matrix for the nanocomposites. Titanium (IV) oxide nanopowder (mixture of rutile and anatase with 99.9% of purity), TiO_2, was purchased from Sigma-Aldrich, with a mean diameter < 100 nm (BET), < 50 nm (XRD) nm and ≈ 75 nm by AFM [20]. Acetone (HPLC grade), from Aldrich, was used as solvent for the solution blow spinning process, SBS.

2.2. Materials preparation

The PMMA/TiO_2 nancomposites with different amounts of TiO_2 (0%, 1%, 2%, 5% and 10% by weight) were prepared in the form of films by SBS using a commercial airbrush (airbrush Elite E7116P) and compressed air. A suspension of TiO_2 nanoparticles in a PMMA solution of 10% wt in a acetone was prepared and then blow spun onto: i) KBr (Sigma-Aldrich) discs of 1 cm of diameter prepared at room temperature by compression at 7 bar for subsequent infrared studies and ii) glass substrates to take from them about 10 mg for thermogravimetric analysis and scanning electron microscopy.

The conditions to perform the SBS were the following:

- Nozzle diameter = 0.5mm.
- Fluid cup capacity = 5 cm^3.
- Pressure = 4 bar.
- Working distance = 16.5 cm.

2.3. Instrumental techniques

Scanning electron microscopy

The morphology in terms of topographic characteristics and the distribution of domains with different elemental composition was imaged using the backscattered electrons, BSE, signal in a Philips XL30 scanning electron microscope. Microanalyses at specific sites on the surfaces were performed with a DX4i coupled energy-dispersive X-ray spectroscopy (EDAX) detector. To avoid charge accumulation the samples were gold coated by sputtering using a low vacuum coater Leica EM ACE200.

Fourier transformed infrared spectroscopy, FTIR

FT-IR analysis was carried out in the transmission mode using a FT-IR Spectrum GX (Perkin-Elmer). Spectra were recorded in the range 400-4000 cm^{-1} from the average of five scans with a resolution of 4 cm^{-1}. Potassium Bromide (KBr) discs were used as substrates of the blow spun materials.

Thermogravimetric analysis

Thermogravimetric analysis, TGA, was carried out with a thermal analyzer Mettler TGA/SDTA851 with multisampler device. All the samples were measured in 50 mL Pt crucibles under nitrogen atmosphere, heating about 2-5 mg from 40 ºC to 800 ºC at 10 ºC/min.

Differential scanning calorimetry

The thermal transitions of PMMA under the influence of TiO_2 nanofiller were studied using a differential scanning calorimeter METTLER Toledo 822E. All samples, of about 1.5-3 mg, were subjected to the following thermal steps under a nitrogen atmosphere: i) a first heating scan from 30º C to 180º C at 20 ºC/min to investigate thermal transitions of the blow spun materials; ii) stabilization step at 180ºC for 5 min to erase thermal history; iii) a cooling scan from 180ºC to 30ºC at 20ºC to study thermal transitions of the relaxed nanocomposite system; and iv) a second heating scan from

30ºC to 180ºC to study the thermal transitions with the same thermal history, avoiding any influence arising from the processing method used.

3. Results and discussion

Representative top surfaces of the blow spun materials are shown in Figures 1 and 2. In each case a relatively flat surface covered with polymeric screw-shaped particles is observed. It is interesting to highlight that, in general, the higher the amount of nanoparticles in the suspension to be blow spun the lower the amount of particles, making the surfaces topographically less heterogeneous. This finding points out that a simple variation of the composition of the suspension to be blow spun may change the surface characteristics of the materials prepared, with implications in their final performance in terms of adhesion phenomena, like wettability, for instance.

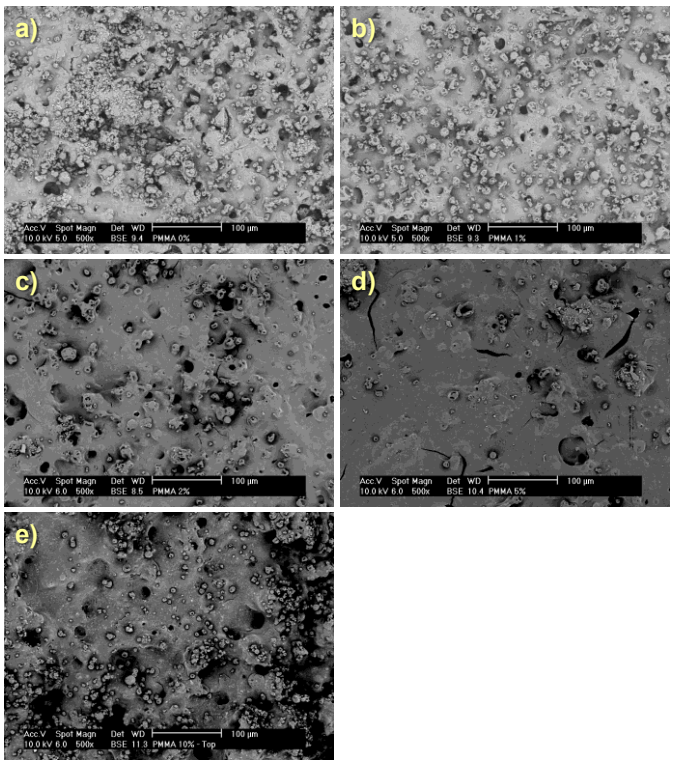

Figure 1. SEM images at low magnification (×500) of the blow spun PMMA/TiO_2 nanocomposites with different amounts of TiO_2 nanoparticles: a) 0%; b)1 %; c) 2%; d) 5% and e) 10% by weight.

SEM images (Figure 1) present small white regions with sizes lower than 800 nm uniform dispersed in a grey matrix (Figure 2), in the samples containing nanoaprticles. Besides, the number of those bright regions increases the higher the amount of TiO_2 in the nanocomposite. In order to better visualize this effect, avoiding the complexity of the topography, an image of the composite with 10% by weight of nanoparticles has been included in Figure 2 (Figure 2f) for which the most flat and smooth surface was inspected by SEM (bottom side, i.e., the surface directly in contact with the glass substrate). Again white small regions well dispersed in a grey matrix are observed. These results suggest that TiO_2 nanoparticles or small aggregates of them are uniformly

dispersed within the PMMA polymer. Additionally, X-ray energy dispersive microanalysis was performed on different regions of the samples observing that, for a chosen white bright region, the corresponding X-ray energy dispersive spectra showed the typical peaks associated to the titanium (Figure 3).

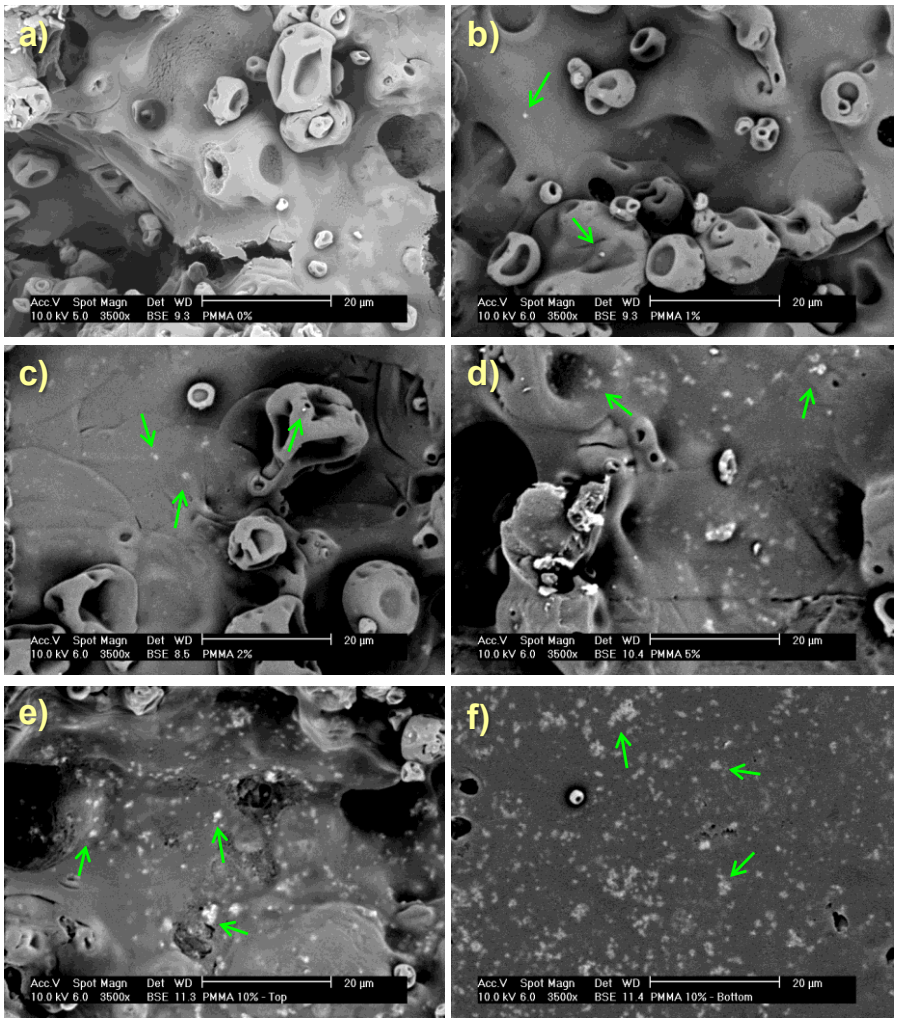

Figure 2. SEM images at high magnification (×2500) of the blow spun PMMA/TiO_2 nanocomposites with different amounts of nanoparticles: a) 0%; b)1 %; c) 2%; d) 5%; e) 10% (top side) and f) 10% (bottom side) by weight.

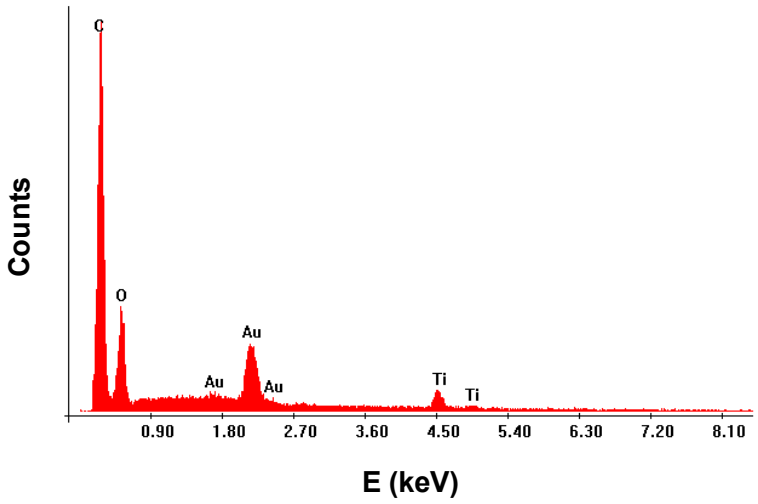

Figure 3. Characteristic X-ray dispersive energy spectra of one of the white regions observed in the SEM images of the composites (Figure 2).

Thus, all these results allow concluding that using SBS it is possible to obtain PMMA/TiO_2 nanocomposites with a relatively high amount of nanoparticles (at least up to 10% wt) uniformly dispersed within the polymeric matrix.

Possible structural variations in the PMMA induced by the SBS process and the presence of TiO_2 nanoparticles were also investigated by FTIR. The vibrational spectra of the blow spun PMMA based materials are shown in Figure 4. As can be seen, only new clear bands at around 668 cm^{-1} appear when the amount of TiO_2 is high enough (2% by weight) that can be assigned to vibration modes of Ti-O-Ti [28]. The rest of bands do not seem to change with respect either to those obtained for commercial PMMA, prepared in different ways [21], or with the amount of TiO_2 nanoparticles present. Thus, neither the SBS process nor the incorporation of TiO_2 nanoparticles seem to greatly affect the PMMA structure, at least under the FTIR sensibility and accuracy. In order to see if specific interactions appear between the TiO_2 nanoparticles and the PMMA A deeper analysis of the FTIR bands should be carried out. For PMMA there are at least four absorption bands in the range between 1050 and 1300 cm^{-1}, assigned to the ester group of poly(methyl methacrylate) [21]. The different possible rotational conformations of the ester group yield different force constants, so variations on the relative absorbances of these peaks are related to the population of the different PMMA conformations. In particular the peaks centered at 1269 cm^{-1} (ν_1) and 124 cm^{-1} (ν_2), are usually assigned to the splitting of ester vibration, ν_a(C-C-O), into two components as a consequence of two rotational-isomeric states, where the C-OCH_3 and C^{α}-CH_3 bonds are in mutual cis or trans orientation arising from the internal C^{α}-CO bond rotation. Therefore, differences in the absorbance ratio between those rotational-isomeric states, A(ν_1)/A(ν_2), should inform about preferential conformations due to specific interactions or forced orientation under particular polymer flow conditions, for example. The calculation of the absorbance ratios from the spectra of Figure 4 yield the following results: 0.72 (PMMA-0%); 0.66 (PMMA-1%); 0.66 (PMMA-2%); 0.68 (PMMA-5%); 0.68 (PMMA-10%). These results point out that due to specific interactions between the ester group and the nanoparticles surface a preferential conformation of the ester group respect to the PMMA backbone is induced which might have influence in the final properties of the materials. Besides it is observed that the addition of just 1% of nanoparticles is enough as to exert the same or even slightly higher influence in the

absorbance ratio $A(\nu_1)/A(\nu_2)$ than higher loaded materials. This can be explained considering the extremely high surface to volume ratio of the nanoparticles so that a small amount of nanoparticles can have enough surface to interact with the ester groups of the PMMA. In the case of higher amounts of nanoparticles, the formation of more number of aggregates might slightly reduce the surface available to interact with the polymer chains. Another way of interpreting these results is by considering that the preferential orientation of the polymer chains induced by the SBS process may be increased when the macromolecules are forced to pass through constrained paths between particles. The reason of decreasing the values of the absorbance ratio for high enough nanoparticles loadings (5% and 10%) may be the formation of aggregates and therefore the existence of wider paths for the macromolecules flow which should lead to less constrained polymer chain motion.

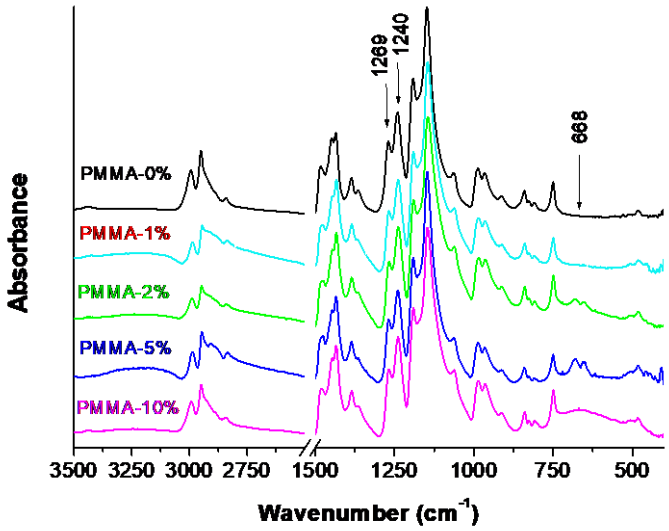

Figure 4. FTIR spectra of the blow spun PMMA based materials with different amounts of TiO_2 nanoparticles (0%, 1%, 2%, 5% and 10% by weight).

The influence of the particular processing by SBS so as the presence of the TiO_2 nanoparticles on the thermal stability of PMMA was also studied by TGA. In Figure 5 the plots of weight loss (top) and the corresponding derivatives (bottom) are shown for all the composites and as sample of commercial PMMA.

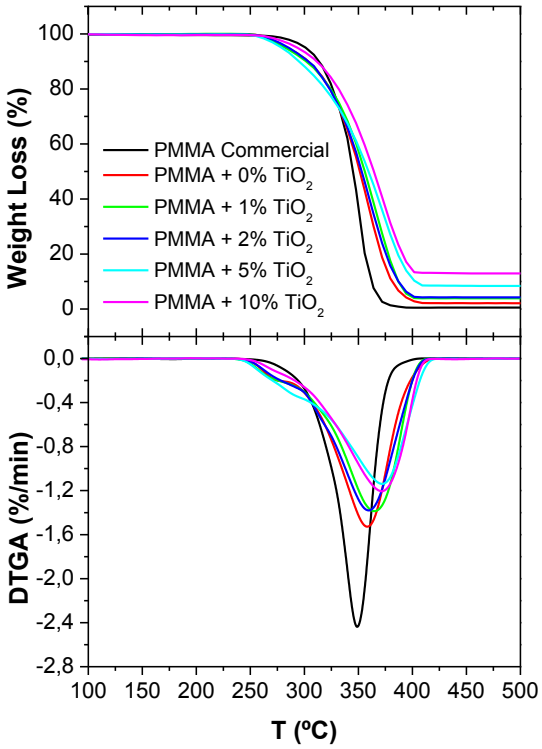

Figure 5. Thermogravimetry, TGA, differential thermogravimetry, DTGA, curves for blow spun PMMA based materials with different amounts of TiO_2 nanoparticles (0%, 1%, 2%, 5% and 10% by weight).

Some alterations in the thermodegradation of PMMA with respect to the blow spinning process can be observed, as well as changes on the decomposition temperature upon the incorporation of TiO_2 nanoparticles. Although the onset of the thermodegradation for the as received PMMA is about 10 ºC higher than the blow spun one, the later presents the maximum rate of degradation at about 10 ºC higher (359 ºC) than that of the as received PMMA (349 ºC). These results are very close to those found between 350-400 ºC for other PMMA samples and that usually are assigned to the random scission of the PMMA backbone [29]. This can be explained considering that the blow spun samples present more surface available being the heat transfer more efficient allowing the thermodegradation process to start before. The second observation might be associated to a small structural change induced by SBS process which must tend to preferentially orient macromolecular chains favouring intermolecular interactions.

On the other hand, it seems that there is a slight influence of the presence of TiO_2 since the temperature of thermodegradation, given by the minimum in the first derivative of the TGA trace, increases with the load of nanoparticles, reaching the highest value, 372 ºC, with the highest amount of TiO_2 (10%). This can be explained considering a dual effect of the filler: a more forced macromolecular chain orientation induced by the presence of the nanoparticle and to the TiO_2 acting as an inorganic barrier protection against the thermodegradation.

In order to study if the process of SBS and the presence of well dispersed TiO_2 exert any influence on the dynamics of the PMMA, differential scanning calorimetry was performed. DSC traces for the first and second heating (after erasing thermal history),

so as for the cooling after the first heating are presented in Figure 6 for all the samples under study. In all cases, a sharp change in the heat flow due to a sharp change in the heat capacity is observed, which is assigned to the glass transition temperature, T_g, of the PMMA. In each case the transition temperature was obtained from the inflexion point of the DSC traces (Table 1). The values obtained are quite closed to those that can be found in the literature for PMMA [9, 21, 30]. As can be seen, regardless the sample, the values of T_g obtained during the first heating are in general slightly higher than those obtained during the second heating. The reason of that might be simply ascribed to the presence of more relaxed polymer after erasing the processing history with less preferentially oriented macromolecules.

For the first heating, when comparing between commercial PMMA and PMMA subjected to the blow spinning process, it can be observed that the later has a slightly higher T_g. This result may be due to induced specific macromolecular chains orientation by the SBS process. This somewhat enhanced local order in the polymer seems to be the cause of a slight higher energy required to induce polymer chain local motions. The values corresponding to the enthalpy relaxation are in agreement with the above mentioned (Table 1). Under the same conditions of DSC measurement, an increased order in a glassy polymer should lead to lower enthalpy relaxation.

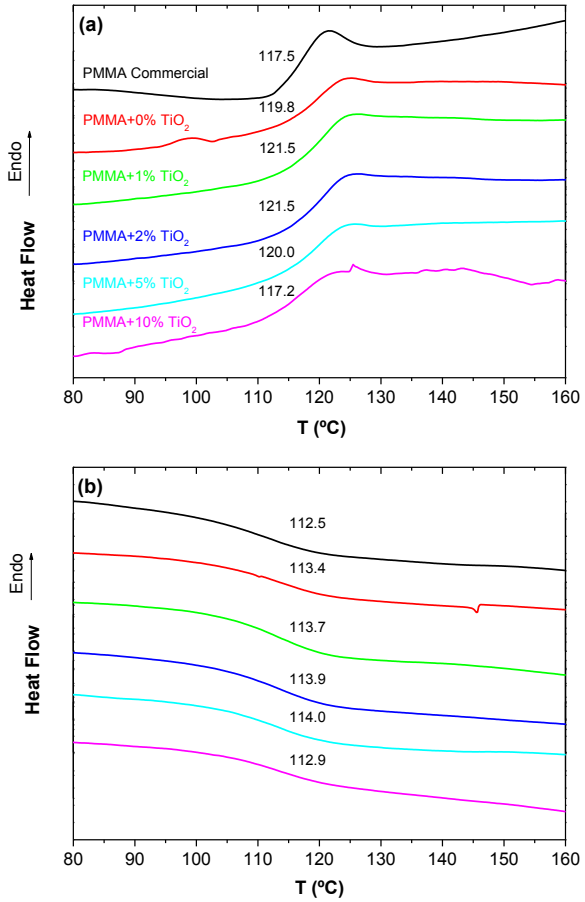

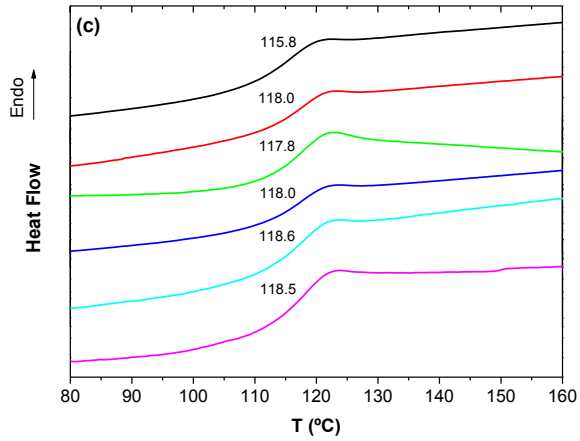

Figure 6. DSC traces of the blow spun PMMA based materials with different amounts of TiO_2 nanoparticles (0%, 1%, 2%, 5% and 10% by weight): a) first heating; b) first cooling and c) second heating.

Table 1. Relaxation enthalpies, ΔH_R, and values of glass transition temperatures obtained from the inflexion points of the DSC curves of the Figure 6.

Sample	Np Content (%5 wt)	T_g (ºC) 1rst Heating	T_g (ºC) 1rst Cooling	T_g (ºC) 2nd Heating	ΔH_R (J/g) 1rst Heating
PMMA Commercial	0	117.5	112.5	115.8	0,306
PMMA-0	0	119.8	113.4	118.0	0.176
PMMA-1	1	121.5	113.7	117.8	0.034
PMMA2	2	121.5	113.9	118.0	0.097
PMMA-5	5	120.0	114.0	118.6	0.146
PMMA-10	10	117.2	112.9	118.5	0.311

For the first heating, when TiO_2 nanoparticles are incorporated to the PMMA the values of T_g tend to increase up to a composition of 2% wt of nanoparticles, changing beyond this point. Besides, the values of relaxation enthalpies follow just the opposite trend (Table 1). In fact when plotting the values of T_g's versus the relaxation enthalpies a linear behavior can be observed (Figure 7). These results suggest that the differences observed between samples about their dynamics are most likely due to a different order degree in the polymer chains induced by the SBS process rather than due to specific interactions between the polymer and the nanoparticles. In fact, these differences disappear after relaxing the system with the first heating, as can be observed in the values of T_g's for the cooling and second heating (Figures 6a and c, and Table 1). A possible explanation for this behavior can be ascribed to the fact that the presence of a certain amount of nanoparticles helps the polymer chains to get oriented during the SBS process when they are forced during the flow to pass through the narrow paths formed by the insurmountable nanoparticles (Figure 8). However, when the amount of nanoparticels is high enough the possibility of forming aggregates would imply wider ways by where the polymer is flowing during the SBS (Figure 8).

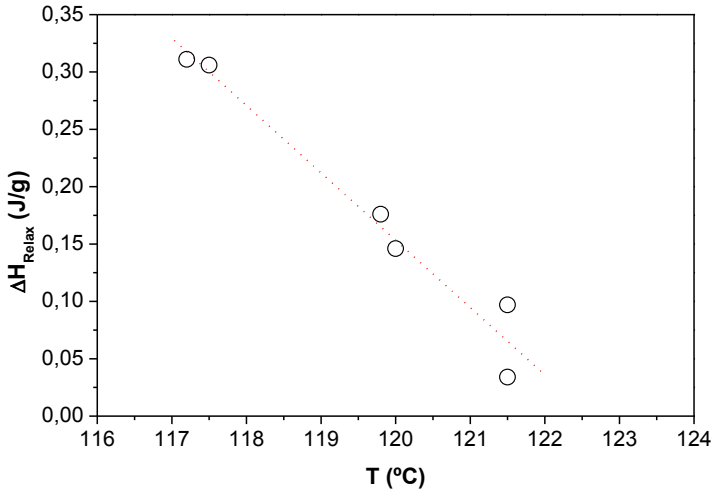

Figure 7. Representation of relaxation enthalpies as a function of the glass transition temperatures.

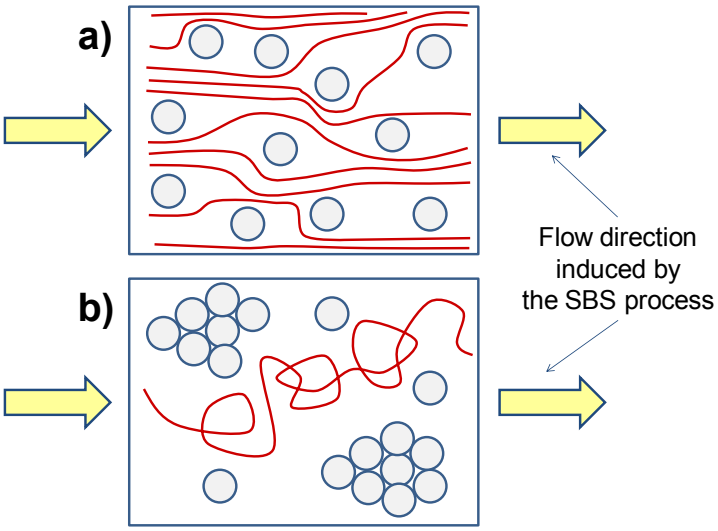

Figure 8. Schematic representation of the possible polymer flow in the composites induced by the SBS process.

4. Conclusions

SBS process was demonstrated to be good to obtain PMMA/TiO_2 nanocomposites with relatively high amount of nanoparticles uniformly dispersed within the polymeric matrix. The simple variation in the composition of the suspension to be blow spun may change the surface characteristics of the materials prepared which might induce their final performance in terms of adhesion phenomena.

It seems that the macromolecular flow forced by the SBS process so as specific interactions between the ester group and the surface of titania nanoparticles induce a

preferential conformation of the ester group respect to the PMMA backbone which improve intermolecular interactions, increasing thermal stability in terms of both macromolecular motion relaxation and degradation.

Acknowledgments

To the memory of Raúl.

Authors gratefully acknowledge financial support from the Project MAT2014-59116-C2 (Ministerio de Economía y Competitividad).

Disclosure of potential conflicts of interest

The authors declare that they have no conflict of interest.

5. References

1. Kuester S, Barra GMO, Ferreira JC, et al (2016) Electromagnetic interference shielding and electrical properties of nanocomposites based on poly (styrene-b-ethylene-ran-butylene-b-styrene) and carbon nanotubes. Eur Polym J 77:43–53. doi: 10.1016/j.eurpolymj.2016.02.020
2. Farhan S, Wang R, Li K (2016) Carbon foam decorated with silver particles and in situ grown nanowires for effective electromagnetic interference shielding. J Mater Sci 51:7991–8004. doi: 10.1007/s10853-016-0068-4
3. Yousefi N, Sun X, Lin X, et al (2014) Highly aligned graphene/polymer nanocomposites with excellent dielectric properties for high-performance electromagnetic interference shielding. Adv Mater 26:5480–5487. doi: 10.1002/adma.201305293
4. Yang M, Dan Y (2005) Preparation and characterization of poly(methyl methacrylate)/titanium oxide composite particles. Colloid Polym Sci 284:243–250. doi: 10.1007/s00396-005-1356-8
5. Zhao H, Li RKY (2006) A study on the photo-degradation of zinc oxide (ZnO) filled polypropylene nanocomposites. Polymer (Guildf) 47:3207–3217. doi: 10.1016/j.polymer.2006.02.089
6. Li YQ, Fu SY, Mai YW (2006) Preparation and characterization of transparent ZnO/epoxy nanocomposites with high-UV shielding efficiency. Polymer (Guildf) 47:2127–2132. doi: 10.1016/j.polymer.2006.01.071
7. González-Benito J, Castillo E, Caldito JF (2013) Coefficient of thermal expansion of TiO 2 filled EVA based nanocomposites. A new insight about the influence of filler particle size in composites. Eur Polym J 49:1747–1752. doi: 10.1016/j.eurpolymj.2013.04.023
8. Olmos D, Martínez F, González-Gaitano G, González-Benito J (2011) Effect of the presence of silica nanoparticles in the coefficient of thermal expansion of LDPE. Eur Polym J 47:1495–1502. doi: 10.1016/j.eurpolymj.2011.06.003
9. Castrillo PD, Olmos D, Amador DR, González-Benito J (2007) Real dispersion of isolated fumed silica nanoparticles in highly filled PMMA prepared by high energy ball milling. J Colloid Interface Sci 308:318–324. doi:

10.1016/j.jcis.2007.01.022
10. Chandra A, Turng LS, Gong S, et al (2007) Study of polystyrene/titanium dioxide nanocomposites via melt compounding for optical applications. Polym Compos 28:241–250. doi: 10.1002/pc.20274
11. Chatterjee U, Jewrajka SK, Guha S (2009) Dispersion of Functionalized Silver Nanoparticles in Polymer Matrices : Stability , Characterization , and Physical Properties. Polymer (Guildf) 30:827–834. doi: 10.1002/pc
12. Ash BJ, Siegel RW, Schadler LS (2004) Mechanical Behavior of Alumina/Poly(methyl methacrylate) Nanocomposites. Macromolecules 37:1358–1369. doi: 10.1021/ma0354400
13. El Achaby M, Arrakhiz F-E, Vaudreuil S, et al (2012) Mechanical, thermal, and rheological properties of graphene-based polypropylene nanocomposites prepared by melt mixing. Polym Compos 33:733–744. doi: 10.1002/pc.22198
14. He JP, Li HM, Wang XY, Gao Y (2006) In situ preparation of poly(ethylene terephthalate)-SiO2 nanocomposites. Eur Polym J 42:1128–1134. doi: 10.1016/j.eurpolymj.2005.11.002
15. Olmos D, Montero F, González-Gaitano G, González-Benito J (2013) Structure and morphology of composites based on polyvinylidene fluoride filled with BaTiO3 submicrometer particles: Effect of processing and filler content. Polym Compos 34:2094–2104. doi: 10.1002/pc.22618
16. Sánchez F a., Redondo M, González-Benito J (2015) Influence of BaTiO3 submicrometric particles on the structure, morphology, and crystallization behavior of poly(vinylidene fluoride). J Appl Polym Sci 132:41497 (1-10). doi: 10.1002/app.41497
17. Olmos D, Martínez-Tarifa JM, González-Gaitano G, González-Benito J (2012) Uniformly dispersed submicrometre BaTiO3 particles in PS based composites. Morphology, structure and dielectric properties. Polym Test 31:1121–1130. doi: 10.1016/j.polymertesting.2012.08.005
18. Gonzalez-Benito J, Martinez-Tarifa J, Sepúlveda-García ME, et al (2013) Composites based on HDPE filled with BaTiO3 submicrometric particles. Morphology, structure and dielectric properties. Polym Test 32:1342–1349. doi: 10.1016/j.polymertesting.2013.08.012
19. Serra-Gómez R, Tardajos G, González-Benito J, González-Gaitano G (2012) Rhodamine solid complexes as fluorescence probes to monitor the dispersion of cyclodextrins in polymeric nanocomposites. Dye Pigment 94:427–436. doi: 10.1016/j.dyepig.2012.02.009
20. Olmos D, Domínguez C, Castrillo PD, Gonzalez-Benito J (2009) Crystallization and final morphology of HDPE: Effect of the high energy ball milling and the presence of TiO2 nanoparticles. Polymer (Guildf) 50:1732–1742. doi: 10.1016/j.polymer.2009.02.011
21. González-Benito J, González-Gaitano G (2008) Interfacial conformations and molecular structure of PMMA in PMMA/silica nanocomposites. Effect of high-energy ball milling. Macromolecules 41:4777–4785. doi: 10.1021/ma800260k
22. E.S. Medeiros, G.M. Glenn, A.P. Klamczynski, W.J. Orts LHCM (2009) Solution blow spinning: a new method to produce micro- and nanofibers from polymer solutions. J Appl Sci 113:2322–2330. doi: 10.1002/app.30275
23. Costa RGF, Brichi GS, Ribeiro C, Mattoso LHC (2016) Nanocomposite fibers of poly(lactic acid)/titanium dioxide prepared by solution blow spinning. Polym Bull 1–13. doi: 10.1007/s00289-016-1635-1
24. Teno J, González-Gaitano G, González-Benito J (2017) Nanofibrous

polysulfone/TiO 2 nanocomposites: Surface properties and their relation with E. coli adhesion. J Polym Sci Part B Polym Phys 55:1575–1584. doi: 10.1002/polb.24404
25. González-Benito J, Teno J, González-Gaitano G, et al (2017) PVDF/TiO2 nanocomposites prepared by solution blow spinning: Surface properties and their relation with S. Mutans adhesion. Polym Test 58:21–30. doi: 10.1016/j.polymertesting.2016.12.005
26. Motaung TE, Luyt AS, Bondioli F, et al (2012) PMMA-titania nanocomposites: Properties and thermal degradation behaviour. Polym Degrad Stab 97:1325–1333. doi: 10.1016/j.polymdegradstab.2012.05.022
27. Motaung TE, Luyt AS, Saladino ML, Caponetti E (2013) Study of morphology, mechanical properties, and thermal degradation of polycarbonate-titania nanocomposites as function of titania crystalline phase and content. Polym Compos 34:164–172. doi: 10.1002/pc.22389
28. Cordeiro D, Vasconcelos L, Costa VC, et al (2011) Infrared Spectroscopy of Titania Sol-Gel Coatings on 316L Stainless Steel. Mater Sci Appl 2011:1375–1382. doi: 10.4236/msa.2011.210186
29. Pantaleón R, González-Benito J (2010) Structure and thermostability of PMMA in PMMA/silica nanocomposites: Effect of high-energy ball milling and the amount of the nanofiller. Polym Compos 31:1585–1592. doi: 10.1002/pc.20946
30. Olmos D, Bagdi K, Mózcó J, et al (2011) Morphology and interphase formation in epoxy/PMMA/glass fiber composites: Effect of the molecular weight of the PMMA. J Colloid Interface Sci 360:289–299. doi: 10.1016/j.jcis.2011.04.028